

Electrically driven silicon resonant light emitting device based on slot-waveguide

Carlos Angulo Barrios

Universidad Politécnica de Valencia, Camino de Vera, s/n, 46022 Valencia, Spain
cbarrios@ntc.upv.es

Michal Lipson

School of Electrical and Computer Engineering, Cornell University, Ithaca, 14840 NY

Abstract: An all-silicon in-plane micron-size electrically driven resonant cavity light emitting device (RCLED) based on slotted waveguide is proposed and modeled. The device consists of a microring resonator formed by Si/SiO₂ slot-waveguide with a low-index electroluminescent material (erbium-doped SiO₂) in the slot region. The geometry of the slot-waveguide permits the definition of a metal-oxide-semiconductor (MOS) configuration for the electrical excitation of the active material. Simulations predict a quality factor Q of 6,700 for a 20- μ m-radius electrically driven microring RCLED capable to operate at a very low bias current of 0.75 nA. Lasing conditions are also discussed.

©2005 Optical Society of America

OCIS codes: (040.6040) Silicon; (130.0130) Integrated Optics; (130.2790) Guided Waves; (130.3120) Integrated Optics Devices.

References and links

1. V. R. Almeida, C. A. Barrios, R. R. Panepucci, and M. Lipson, "All-optical control of light on a silicon chip," *Nature* **431**, 1081-1084 (2004).
2. A. S. Liu, R. Jones, L. Liao, D. Samara-Rubio, D. Rubin, O. Cohen, R. Nicolaescu, and M. Paniccia, "A high-speed silicon optical modulator based on a metal oxide-semiconductor capacitor," *Nature* **427**, 615-618 (2004).
3. Q. Xu, B. Schmitdt, S. Pradhan, and M. Lipson, "Micrometre-scale silicon electro-optic modulator," *Nature* **435**, 325-327 (2005).
4. K. D. Hirschman, L. Tsybeskov, S. P. Dutta-gupta and P. M. Fauchet, "Silicon-based visible light-emitting devices integrated into microelectronics circuits," *Nature* **348**, 338-341 (1996).
5. R. J. Walters, G. I. Bourianoff and H. A. Atwater, "Field-effect electroluminescence in silicon nanocrystals," *Nature Materials* **4**, 143-146 (2005).
6. O. Boyraz and B. Jalali, "Demonstration of a silicon Raman laser," *Opt. Express* **12**, 5269-5273 (2004), <http://www.opticsexpress.org/abstract.cfm?URI=OPEX-12-21-5269>.
7. H. Rong, R. Jones, A. Liu, O. Cohen, D. Hak, A. Fang, and M. Paniccia, "A continuous-wave Raman silicon laser," *Nature* **433**, 725-728 (2005).
8. M. E. Castagna, S. Coffa, M. Monaco, A. Muscara, L. Caristia, S. Lorenti, and A. Messina, "High efficiency light emitting devices in silicon," *Mater. Sci. Eng. B* **105**, 83-90 (2003).
9. V. Almeida, Q. Xu, C. A. Barrios, and M. Lipson, "Guiding and confining light in void nanostructure," *Opt. Lett.*, **29**, 1209-1211 (2004).
10. T. Baehr-Jones, M. Hochberg, C. Walker, A. Scherer, "High-Q optical resonators in silicon-on-insulator-based slot waveguides," *Appl. Phys. Lett.* **86**, 081101 (2005).
11. C. A. Barrios, V. R. A. R. Panepucci and M. Lipson, "Electrooptic modulation of silicon-on-insulator submicrometer-size waveguide devices," *J. Lightwave Technol.* **21**, 2332-2339 (2003).
12. <http://www.rsoftinc.com/fullwave.htm>
13. A. Yariv, "Universal relations for coupling of optical power between microresonators and dielectric waveguides," *Electron. Lett.*, **36**, 321-322 (2000).
14. R. A. Soref and B. R. Bennett, "Kramers-Kronig analysis of E-O switching in silicon," *SPIE Integr. Opt. Circuit Eng.*, **704**, 1986.
15. P. G. Kik and A. Polman, "Erbium doped optical waveguide amplifiers on silicon," *Materials Research Society Bulletin* **23**(4), 48 (1998).

16. SILVACO International. 4701 Patrick Henry Drive, Bldg.1, Santa Clara, CA 94054.
 17. M. Lipson, T. Chen, K. Chen, X. Duan, and L. C. Kimerling, "Erbium in Si-based light confining structures," *Mater. Sci. Eng. B* **81**, 36-39 (2001).
 18. A. Polman, B. Min, J. Kalkman, T. J. Kippenberg, and K. J. Vahala, "Ultra-low threshold erbium-implanted toroidal microlaser on silicon," *Appl. Phys. Lett.* **84**, 1037-1039 (2004).
 19. P. Koonath, T. Indukuri, and B. Jalali, "Vertically-coupled micro-resonators realized using three-dimensional sculpting in silicon," *Appl. Phys. Lett.* **85**, 1018-1020 (2004).
 20. L. Liao, D. Samara-Rubio, M. Morse, A. Liu, D. Hodge, D. Rubin, U. D. Keil, and T. Franck, "High speed silicon Mach-Zehnder modulator," *Opt. Express*, **13**, 3129-3135 (2005).
<http://www.opticsexpress.org/abstract.cfm?URI=OPEX-13-8-3129>
 21. M. K. Emsley, O. Dosunmu, and M. S. Ünlü, "Silicon substrates with buried distributed Bragg reflectors for resonant cavity-enhanced optoelectronics," *IEEE J. Selected Top. Quantum Electron.* **8**, 949-955 (2002).
 22. M. Gnan, H. M. H. Chong, S. S. Kim, A. C. Bryce, M. Sorel, and R. M. De La Rue, "Coupled microcavity in photonic wire Bragg grating," *Conference on Lasers and Electro Optics (CLEO)*, paper CWG7, San Francisco, 2004.
 23. J. T. Robinson, C. Manolatu, L. Chen, and M. Lipson, "Ultrasml modal volumes in dielectric optical microcavities," *Phys. Rev. Lett.*, **95**, 143901 (2005).
-

1. Introduction

Recent breakthroughs [1-7] have boosted the interest in Si microphotonics as a technology for integrating optical and electronic components on a single Si chip. In particular, the demonstration of a continuous-wave optically-pumped Si laser [7] has been of special relevance. However, such a device is optically-pumped and emits at 1.686 μm wavelength, limiting its practical applications. An electrically-driven Si light emitting device (LED) is desirable since it can be considered as the natural interface between photonics and electronics. In addition, emission at 1.55- μm -wavelength is also required for applications in the telecommunication field.

Among the different approaches for achieving an electrically-pumped Si-based light emitting material at 1.55 μm compatible with the CMOS technology, Erbium (Er)-doped SiO_2 has been shown to be a promising option [8]. Si LEDs based on metal-oxide-semiconductor (MOS) structures with Er implanted in the thin gate oxide have shown external quantum efficiencies as high as 10%, which is comparable to that of standard III-V semiconductors LEDs. By current injection through the MOS structure, energetic (hot) electrons can excite Er ions by impact ionization and generate electroluminescence at 1.54 μm .

An optical cavity can increase the brilliance of a LED and it is an essential element for a laser. In order to be employed with the aforementioned Er-doped SiO_2 active material for on-chip applications, an optical cavity should: 1) permit electrical injection, 2) present a high optical mode-active material overlap, 3) be made of CMOS-compatible materials, 4) be micron-size, and 5) exhibit a high quality-factor Q. A planar waveguide-based cavity, such as a ring resonator, is a good choice for this purpose since it can provide a long light-matter interaction path. However, Er-doped SiO_2 has low refractive index and, therefore, a conventional strip waveguide using this material as the core would present two important drawbacks: a) waveguides would require a large cross-section area, which makes difficult current injection through the thick oxide, and b) the low-index-contrast system SiO_2/air does not facilitate miniaturization.

A novel guided-wave slot structure, first proposed in Ref. [9], overcomes the aforementioned drawbacks. This waveguide enables to concentrate a large fraction of the guided mode into a thin low-index layer (slot) sandwiched between two high-index strips. Thus, if the slot-waveguide geometry consists of two doped Si strips (electrodes), sandwiching a thin Er-doped- SiO_2 slot layer (gate oxide), current injection through the gate oxide can be achieved, generating light in the oxide-slot region where the guided-mode is strongly confined. Thus, the aforementioned requisites 1, 2 and 3 are fulfilled. The feasibility of requisites 4 and 5 has been demonstrated in [10], reporting 50- μm -diameter high-Q ($\sim 20,000$) optical resonators in silicon-on-insulator based on slot-waveguides with losses as

Thus, the optical structure is also a MOS configuration that enables current injection through the gate Er-doped oxide (slot). SiO₂ covers the whole device. A practical realization of the proposed structure may involve two etching steps: first, the slot can be etched down to the BOX, as achieved in Ref. [10], and second, after a lithographic process, the Si device layer can be partially etched in order to leave a thin slab of Si for electrical contacts, as demonstrated in Ref. [3]. The gate oxide could be either thermally grown, by proper optimization of the oxidation temperature, or deposited by using a low deposition rate technique such as low pressure chemical vapor deposition (LPCVD). After the formation of the oxide gate, Er ion implantation can be carried out with a posterior thermal annealing for the activation of the Er ions [8].

The optical mode characteristics of the slot-waveguide were calculated by employing the beam propagation method (BPM) [12]. The transmission characteristics of the bus-coupled microring were calculated by using the transfer matrix method [13]. The refractive indexes of undoped Si and SiO₂ (Er-doped SiO₂) were assumed to be 3.48 and 1.46, respectively. The real refractive index and absorption coefficient of the doped Si regions due to the free-carrier dispersion are calculated by using the relations [14]:

$$\Delta n = \Delta n_e + \Delta n_h = -[8.8 \times 10^{-22} \cdot \Delta N + 8.5 \times 10^{-18} \cdot (\Delta P)^{0.8}] \quad (1)$$

$$\Delta \alpha = \Delta \alpha_e + \Delta \alpha_h = 8.5 \times 10^{-18} \cdot \Delta N + 6.0 \times 10^{-18} \cdot \Delta P \quad (2)$$

where

Δn_e is the refractive index change due to electron concentration change;

Δn_h is the refractive index change due to hole concentration change;

ΔN is the electron concentration change in cm⁻³;

ΔP is the hole concentration change in cm⁻³;

$\Delta \alpha_e$ (in cm⁻¹) is the absorption coefficient variations due to ΔN ;

$\Delta \alpha_h$ (in cm⁻¹) is the absorption coefficient variation due to ΔP .

The self-absorption coefficient in the Er-doped SiO₂ region has been assumed to be 0.1 cm⁻¹, that is 0.43 dB/cm, which results from the product of typical values for the absorption cross section and ion concentration, 10⁻²⁰ cm² and 10¹⁹ cm⁻³, respectively, of erbium in SiO₂. [15].

A two-dimensional (2-D) semiconductor device modeling software, ATLAS from SILVACO [16], was employed to calculate the dc electric-field across the gate oxide of the biased structures.

3. Results and discussion

3.1 Optical characteristics

Figure 2 shows the optical field distribution for the quasi-TE (major E-field component perpendicular to the Si/slot interface) for the proposed slot-waveguide. The operating wavelength is 1.54 μm. The optical field is strongly confined in the low-index slot region. The normalized power in the slot (with respect to the total power in the waveguide) was estimated to be around 30%. The effective refractive index was calculated to be $n_{\text{eff}} = 1.99 + j9.7 \times 10^{-6}$. The imaginary part of n_{eff} represents an absorption coefficient of $\alpha_{\text{fc}} = 3.4$ dB/cm. Note that the latter value is smaller than the bulk material losses (due to free-carrier absorption) exhibited by the doped ($P = 10^{18}$ cm⁻³) Si rails (6 dB/cm). This is because only a small fraction of the optical mode is located in the highly lossy Si regions, as revealed in Fig. 2. As a consequence of this small overlap between the doped regions and the optical field, the imaginary part (transmission loss) of the effective refractive index of the waveguide becomes smaller than the bulk doped-Si material losses. This is a unique feature of the slot-waveguide that enables to place high-index lossy materials (for example, highly doped semiconductors

for defining electrodes) close to the maximum value of the guided optical field without introducing excessive optical losses, which is especially useful in the design of high performance electro-optic devices.

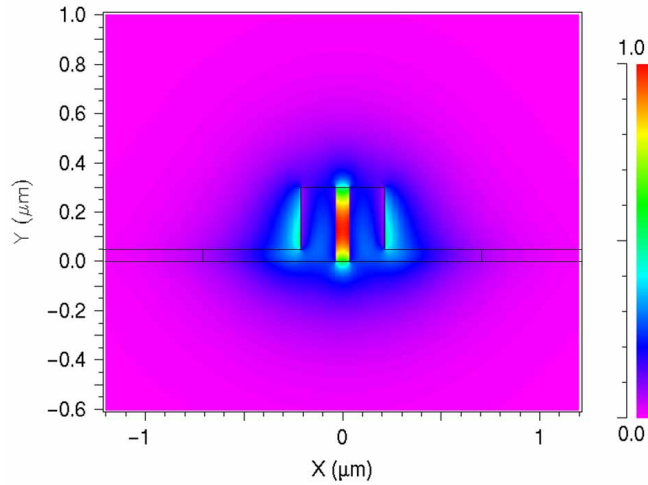


Fig. 2. Transverse E-field amplitude (contour) of the quasi-TE optical mode.

Figure 3 shows the quasi-TE optical mode distribution in a bent slot-waveguide turning to the left (-x axis) with a radius of curvature of 20 μm . It is seen that the optical field is still strongly concentrated in the slot region and slightly shifts to the right side (+x axis) due to the bending effect. Bending radiation losses (α_{bend}) were calculated by monitoring the optical power of the quasi-TE mode in the bent waveguide as a function of the propagation distance, resulting radiation losses of 2.25 dB/cm for a radius of curvature of 20 μm . This radius value has been chosen as a trade-off between low radiation losses and short ring length. Low radiation losses are necessary in order to achieve a high cavity quality factor; however an excessively large radius (long optical path) would enhance the effect of the optical losses and reduce the output power.

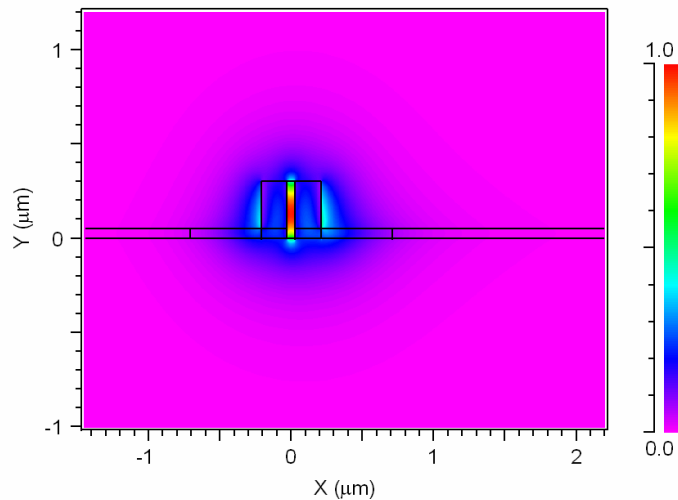


Fig. 3. Transverse E-field amplitude (contour) of the quasi-TE optical mode for a bent slot-waveguide turning to the left (-x axis) with a radius of curvature of 20 μm .

In order to estimate the performance of the microring resonator illustrated in Fig. 1(a), the following parameters were used: radius (R) = 20 μm , power-coupling coefficient ($|\kappa|^2$) = 0.1, and optical losses $\alpha = \alpha_{\text{scat}} + \alpha_{\text{fc}} + \alpha_{\text{bend}}$. α_{scat} represents the optical losses in the slot-waveguide due to scattering at the sidewalls of the Si rails, which has been experimentally determined to be ~ 10 dB/cm [10]. Thus, $\alpha = 15.6$ dB/cm and the total internal loss in the ring, $A_i = \alpha 2\pi R = 0.2$ dB. The ring radius must satisfy the condition $2\pi R = m(\lambda_e/2n_{\text{eff}})$, where m is an integer, in order to have a resonance at the emission wavelength $\lambda_e = 1540$ nm. Figure 4 shows the transmittance characteristics of the microring. The calculated quality factor Q , defined as the ratio of the resonance frequency (ω_r) to the full width at half maximum of the resonance ($\Delta\omega$), is $Q = \omega_r/\Delta\omega = 6.7 \times 10^3$. This value is one order of magnitude higher than that exhibited by vertical Fabry-Perot cavities formed by multilayer Si/SiO₂ Distributed Bragg Reflectors (DBR) [17]. Note that the calculated Q corresponds to a passive ring; if optical gain is achieved in the active material a narrower resonance peak, and higher Q , could be obtained [13].

Laser oscillation would occur if the following condition is satisfied: $(\Gamma g - \alpha)L = -\ln(1 - |\kappa|^2)$, where Γ is the confinement factor, L is the length of the ring and g the active material gain. If a low value of $|\kappa|^2$ such as 0.025 is used in order to increase the ring Q and decrease the factor $-\ln(1 - |\kappa|^2)$, the modal gain equals $\Gamma g = 5.7 \text{ cm}^{-1}$ for a ring radius of $R = 20 \mu\text{m}$. Since $\Gamma = 0.3$, the active material optical gain needed for lasing would be $g = 19 \text{ cm}^{-1}$. Although this value can be reduced by increasing the ring radius, that is, the active region length, the condition $\Gamma g > \alpha = 3.64 \text{ cm}^{-1}$ must be always satisfied. At present, the material system Er³⁺ in SiO₂ has exhibited optical gain when optically pumped [15, 18], and the maximum total gain achieved so far (around 0.14 cm^{-1} [15]) is much smaller than the calculated here. Nevertheless, the high values of cross section of excitation obtained by electrical pumping of Er³⁺ in SiO₂ [8] suggest that higher gains can be achieved by electrical excitation. In any case, for lasing, the waveguide losses must be significantly reduced through improvements in the processing of the slot-waveguides in order to reduce scattering, which is estimated to be the main source of loss in the proposed structure. The feasibility of laser emission in Er-doped SiO₂ microcavities has been demonstrated by Polman et al. [18] by using low loss toroidal microresonators. The smooth surface of the SiO₂ toroidal resonator resulting from the fabrication procedure permits to reduce significantly scattering losses allowing lasing by using small optical pump power.

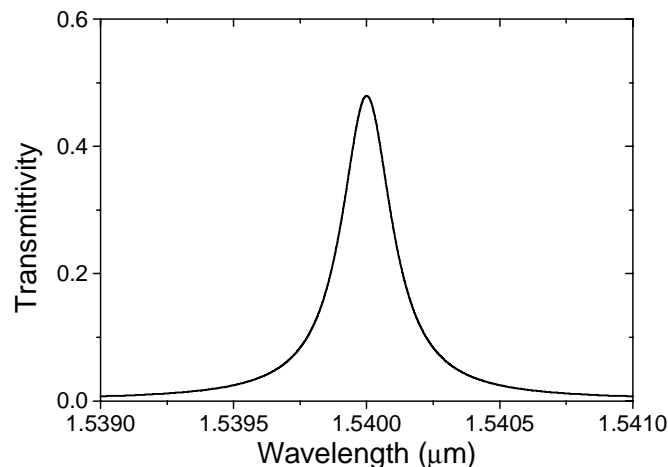


Fig. 4. Calculated spectral transmittance of the ring resonator shown in Fig. 1(a). The quality factor Q is 6,700.

3.2 Electrical characteristics

Carrier transport through the gate oxide in the studied device can be attributed to Fowler-Nordheim (F-N) tunneling [8], which depends on the barrier height between Si and SiO₂ and the applied electric field (E) across the oxide. For F-N tunneling, the E-field across the slot oxide must be in the range of 7.5 MV/cm to 10 MV/cm (breakdown voltage of oxide), that is, between 45 V and 60 V. Figure 5 shows the 2-D distribution of the dc electric field for an applied voltage ($V_{\text{anode}} - V_{\text{cathode}}$) of 55 V. The transverse electric field in the slot region is nearly uniform and most of the applied voltage drops across the Er-doped SiO₂. This assures a uniform current injection through the gate oxide. The experimental value of the F-N current density needed to produce electroluminescence saturation (maximum concentration of excited Er ions) in Er-doped SiO₂ MOS devices is $J = 2 \text{ mA/cm}^2$ [8], therefore the bias current for the slot-waveguide ring LED would be $I = J \cdot A_{\text{ring}} = (2 \text{ mA/cm}^2) \cdot (2\pi \cdot 20 \mu\text{m} \cdot 0.3 \mu\text{m}) = 0.75 \text{ nA}$, where A_{ring} is the area of the vertical surface of the active region (slot). Thus, if the needed voltage to achieve such a current density is 55 V, the power consumption would be only 41.2 nW. This small power consumption arises from the small area of the active region.

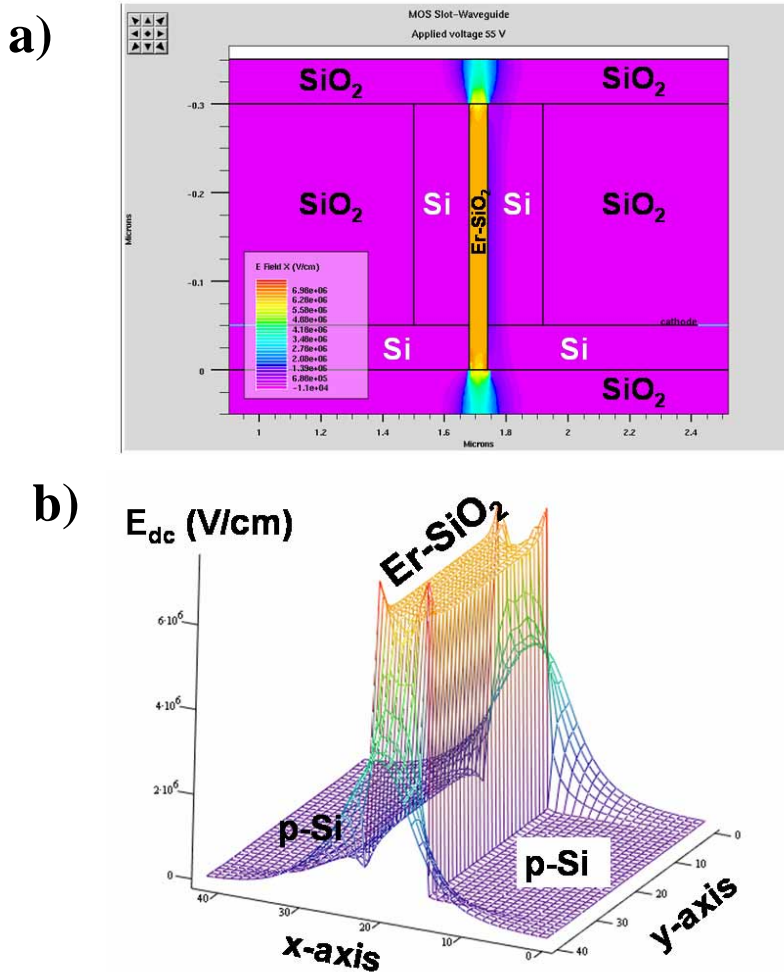


Fig. 5. (a) 2-D distribution of the applied electric field for a bias voltage of 55 V. (b) 2-D profile of the applied electric field.

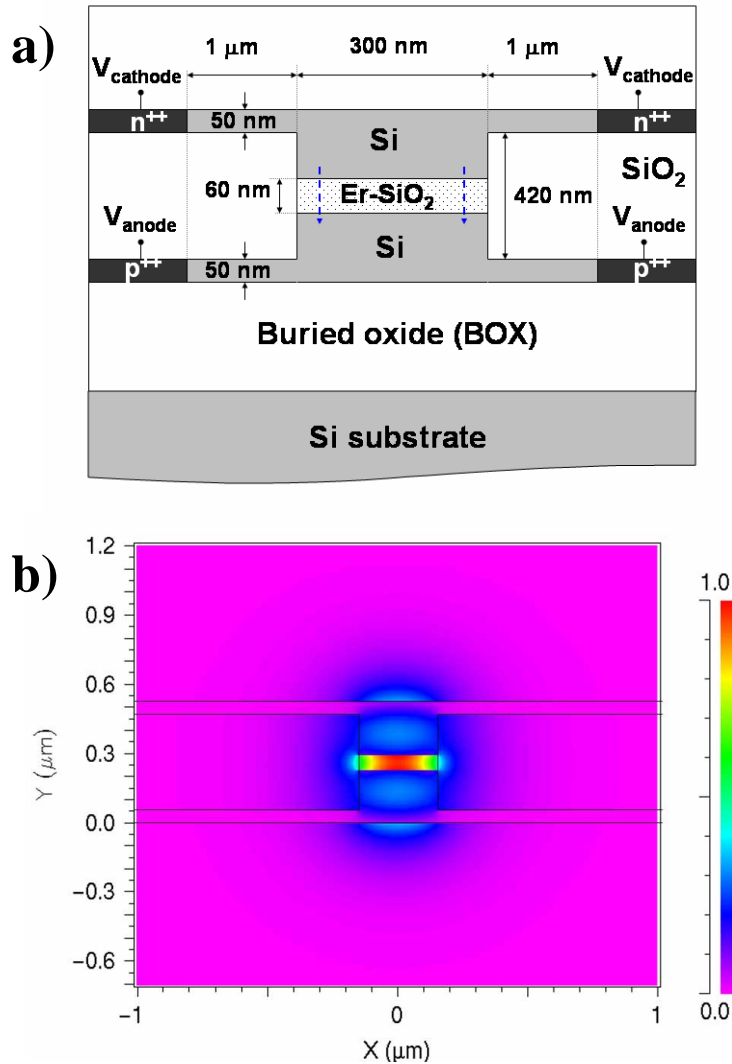


Fig. 6. (a) Schematic cross-sectional view of a horizontal MOS slot-waveguide. The dashed blue arrows indicate the flow of injected electrons through the active gate oxide. (b) Transverse E-field amplitude (contour) of the quasi-TM optical mode.

3.3 Other configurations

It should be mentioned that, besides the vertical slot-waveguide configuration of Fig. 1(b), a horizontal configuration as that shown in Fig. 6(a) could be also used. In this case, the device would operate under quasi-TM polarization (major E-field component perpendicular to the Si/slot interface), as illustrated in Fig. 6(b). The complex refractive index of the slot-waveguide shown in Fig. 6(a) was calculated to be $n_{\text{eff}}=2.16+j1.21 \times 10^{-5}$, which corresponds to an absorption coefficient of 3.9 dB/cm. This value is slightly larger than that exhibited by the vertical configuration due to the presence of more doped Si regions. The horizontal configuration can be advantageous in order to reduce scattering losses induced by imperfections at the Si/SiO₂ interfaces. This is because a horizontal slot-waveguide could be fabricated by ion implantation (oxygen [19] and erbium ions [8]), poly-Si deposition, lateral overgrowth epitaxy [20] and wafer bonding [21] techniques, which would lead to much

smoother interfaces than that produced by reactive ion etching techniques, used for the fabrication of vertical slot-waveguides [10]. The reduction of scattering losses would be of great importance in order to achieve laser emission, as shown in [18]. In addition, a horizontal configuration would enable the implementation of rings with smaller radius of curvature since the width of the Si rails (along the x-axis) forming the horizontal slot-waveguide is larger than that of the Si rails in a vertical configuration, and therefore, the optical field is more confined (lower radiation losses) in the Si regions of the horizontal structure than in those of the vertical one when the waveguide is bent in the plane of the device.

Finally, it should be noted that, besides a microring resonator, a Fabry-Perot (F-P) microcavity defined by DBRs, as that shown schematically in Fig. 7, could be considered for optical feedback. Similar F-P cavities based on conventional strip photonic wire have been demonstrated on SOI substrates, exhibiting $Q > 1400$ [22]. A F-P cavity would be advantageous in order to create a RCLED based on the Purcell effect, since extremely small modal volumes can be obtained [23], whereas the modal volume in a ring resonator is limited by the minimum tolerable radius of curvature before the optical mode in the bend is not guided and gets radiated. Thus, it can be stated that a F-P resonator is ideal to get small modal volumes (which is good for Purcell effect-based devices), whereas a ring (or disk) resonator is an excellent structure for achieving high quality factors (which is good for increasing LED brilliance and obtain laser emission).

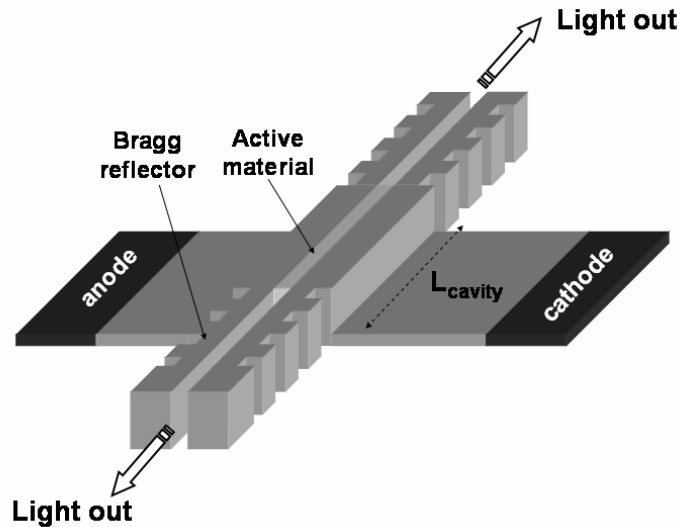


Fig. 7. Fabry-Perot microcavity LED based on a slot-waveguide. Two DBRs defined the resonant structure. A MOS diode is defined in the cavity region for electrical pumping of the active material.

4. Conclusions

A novel in-plane Si electrically-driven RCLED based on a Si/SiO₂ slot-waveguide microresonator with electroluminescent Er-doped SiO₂ in the slot region has been proposed. The geometry of the slotted waveguide permits the definition of a MOS diode for the electrical excitation of the active material. The small percentage of the optical mode contained in the doped Si rails enables to reduce waveguide losses due to free-carrier absorption. On the other hand, the high percentage of the optical mode contained in the electroluminescent slot-region allows for high interaction between the active material and the guided light. Simulations indicate that a microresonator based on the MOS-slot configuration is capable to exhibit a quality factor of 6,700 and it is able to emit light at 1.54 μm with a bias current of

only 0.75 nA. With further improvements in processing and active materials, the proposed electro-optical slot-waveguide-based resonant architecture may be a promising candidate for the fabrication of an electrically-pumped Si laser.

Acknowledgments

This work was supported by the Spanish Ministry of “Educación y Ciencia” under Program “Ramón y Cajal”, the Cornell Center for Nanoscale Systems, the Cornell Center for Material Research (CCMR grant M23-8494), and the National Science Foundation's CAREER Grant No. 0446571. The authors would also like to thank Gary Tompa of Structured Materials Industries, Inc. and Gernot Pomrenke from the Air Force Office of Scientific Research for supporting the work under grant number FA9550-05-C-0102.